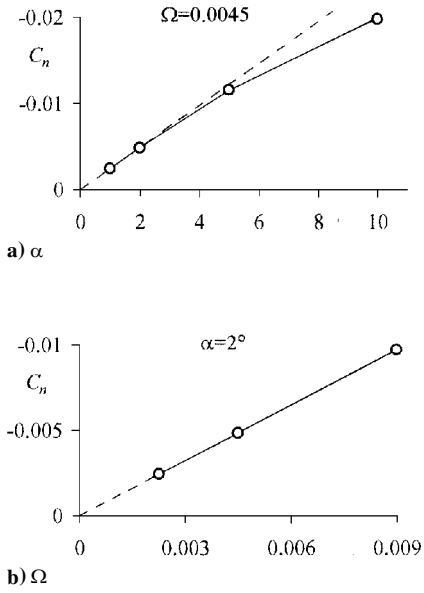

Fig. 4 Variation of side moment coefficient for CAN4 geometry undergoing lunar coning motion, $M = 5.725$ and $Re = 2.3 \times 10^6$.

changes in the PDC sum can be obtained by varying the c.g. position.

The calculation of PDCs from moment expansions is based on the assumption that forces and moments vary linearly with incidence and angular rate. The effect of angle of incidence and angular rate on the calculated side moment coefficient C_n have therefore been investigated. From Fig. 4a, it is observed that the side moment may only be considered as a linear function of incidence over a very small range of incidences below 5 deg. In Fig. 4b, side moment is seen to vary linearly with angular rate at least up to rates of 0.009. It is concluded that the parameters used in the present investigation lie within the region of linear behavior, and so the use of moment expansions is valid.

Acknowledgment

This research was supported by the Defence Research Agency under Contract WSS/V1392.

References

[1]Schiff, L. B., "A Study of the Nonlinear Aerodynamics of Bodies in Nonplanar Motion," NASA TR R-421, Jan. 1974.

[2]Murphy, C. H., "Free Flight Motion of Symmetric Missiles," U.S. Army Ballistic Research Lab., Rept. 1216, Aberdeen Proving Ground, MD, July 1963.

[3]Levy, L. L., and Tobak, M., "Nonlinear Aerodynamics of Bodies of Revolution in Free Flight," *AIAA Journal*, Vol. 8, No. 12, 1970, pp. 2168–2171.

[4]Schiff, L. B., and Tobak, M., "Results from a New Wind-Tunnel Apparatus for Studying Coning and Spinning Motions of Bodies of Revolution," *AIAA Journal*, Vol. 8, No. 11, 1970, pp. 1953–1957.

[5]Weinacht, P., Sturek, W. B., and Schiff, L. B., "Navier–Stokes Predictions of Pitch Damping for Axisymmetric Shell Using Steady Coning Motion," AIAA Paper 91-2855, Aug. 1991.

[6]Weinacht, P., "Navier–Stokes Predictions of the Individual Components of the Pitch-Damping Coefficient Sum," AIAA Paper 95-3485, Aug. 1995.

[7]Qin, N., Ludlow, D. K., Shaw, S. T., Edwards, J. A., and Dupuis, A., "Calculation of Pitch Damping Coefficients for Projectiles," AIAA Paper 97-0405, Jan. 1997.

[8]Dupuis, A., and Edwards, J. A., "Aeroballistic Range Tests of the CAN4 Projectile at Hypersonic Velocities," 21st TTCP WTP2 Meeting, Salisbury, Australia, April 1996.

R. M. Cummings
Associate Editor

Individual Components of the Yaw Damping Sum: Implementation for Tumbling Bodies

S. Ellis,* L. W. Longdon,† and G. M. Moss‡
Cranfield University, Shrivenham, Swindon SN6 8LA, Wiltshire, England, United Kingdom

Nomenclature

G	= body center of gravity
m	= mass of body
p, q, r	= components of body angular velocity about x, y, and z axes, respectively
Q	= direction of $\boldsymbol{R}$ relative to y axis in y–z plane, $\tan^{-1}(r/q)$
R'	= radius of planar loop
$\boldsymbol{R}$	= body rotation vector in y–z plane
S	= direction of $\dot{\alpha}$ relative to y axis in y–z plane
t	= time
u, v, w	= components of body linear velocity along x, y, and z axes, respectively
$\boldsymbol{V}$	= body linear velocity vector, $u\hat{\boldsymbol{\xi}} + v\hat{\boldsymbol{\eta}} + w\hat{\boldsymbol{\zeta}}$
XF, YF, ZF	= body forces in x, y, and z directions, respectively
x, y, z	= body coordinate axes
$\dot{\alpha}$	= heave component of $\mathrm{d}\sigma/\mathrm{d}t$
λ	= roll angle
$\hat{\boldsymbol{\xi}}, \hat{\boldsymbol{\eta}}, \hat{\boldsymbol{\zeta}}$	= unit vectors in x, y, and z directions, respectively
σ	= total incidence
$\boldsymbol{\omega}$	= body angular velocity vector, $p\hat{\boldsymbol{\xi}} + q\hat{\boldsymbol{\eta}} + r\hat{\boldsymbol{\zeta}}$

Subscript

e	= relative to Earth-fixed reference system

Introduction

PARTLY because of the difficulty of arriving at separate values for the individual pitch damping derivatives C_{M_q} and $C_{M_{\dot{\alpha}}}$ in external ballistic calculations, it is normal to combine the derivatives C_{M_q} and $C_{M_{\dot{\alpha}}}$ in a single term C_q (for example, Ref. 1).

Fairly recently, Weinacht[2] gave an innovative computational fluid dynamics (CFD) technique for the separate estimation of these q and $\dot{\alpha}$ dependent coefficients for a projectile in flight. That study is most likely the first time that such a predictive capability has been achieved.

If the results from such an analysis are to be useful, they need to be incorporated into an analytical model of the motion of the projectile. For normal projectile trajectory modeling, this is not strictly necessary as q and $\dot{\alpha}$ are essentially equivalent. Additionally, for linearized models, this incorporation is relatively straightforward, but the linearization process does not then make full use of the predictive potential of the CFD solutions.

This Note relates to the implementation of the separate treatment of these two motions into a full six-degree-of-freedom model, which does not contain small angle assumptions. It can therefore utilize the full potential of the CFD predictions because there are no limits on the attitude angles of the projectile. It was found that this implementation required some additional analysis; its development and use are described in this Note.

Received Jan. 2, 1997; revision received May 7, 1997; accepted for publication May 14, 1997.

*Principal Research Officer, Ballistics Group, Royal Military College of Science.

†Consultant, School of Engineering and Applied Science, Royal Military College of Science.

‡Senior Lecturer, Department of Aerospace and Guidance Systems, Royal Military College of Science.

Our basic assumption is that heave (referred to here as the $\dot{\boldsymbol{\alpha}}$ motion) and the body rotation in the cross-flow plane (referred to as the $\boldsymbol{R}$ motion) are the only two components of the rate of change of total incidence. This premise is used to deduce the magnitude and direction of $\dot{\boldsymbol{\alpha}}$ by equating them to the properties of the vector, which is the difference between the vector rate of change of total incidence and the body rotation vector in the body cross-flow plane. (Note that, in general, heave is actually composed of elements of both heave and swerve and, from this analysis, which uses a body-fixed, rotating coordinate system, body rotation as well.) Note also that the ballistics convention of using yaw to describe incidence angles regardless of roll attitude is implicit here.

Rate of Change of Total Incidence

The full six-degree-of-freedom model is based on the equations of motion for a nonaxisymmetric rigid body with six degrees of freedom.[3] The model was designed to simulate the postricochet flight of a spinning projectile that had been deformed in the ricochet process, had a residual axial spin, and was tumbling.

In these circumstances, to adequately describe the motion we need a model expressed in body axes. It is convenient to work in terms of the total incidence angle σ, which is the angle between the velocity vector and the body longitudinal axis and lying in the plane defined by the roll angle λ (Fig. 1).

To obtain an expression for the total incidence rate $\mathrm{d}\sigma/\mathrm{d}t$ we differentiate the expression

$$\cos\sigma = \frac{(\boldsymbol{V}\cdot\hat{\boldsymbol{\xi}})}{|\boldsymbol{V}|} \tag{1}$$

with respect to t to give

$$-\sin\sigma\frac{\mathrm{d}\sigma}{\mathrm{d}t} = \frac{[(\mathrm{d}\boldsymbol{V}/\mathrm{d}t)\cdot\hat{\boldsymbol{\xi}}]}{|\boldsymbol{V}|} + \frac{[\boldsymbol{V}\cdot(\mathrm{d}\hat{\boldsymbol{\xi}}/\mathrm{d}t)]}{|\boldsymbol{V}|} - \frac{(\boldsymbol{V}\cdot\hat{\boldsymbol{\xi}})\cdot\mathrm{d}|\boldsymbol{V}|/\mathrm{d}t}{|\boldsymbol{V}|^2} \tag{2}$$

Because the body axis system is rotating about G with angular velocity $\boldsymbol{\omega}$, we have

$$\frac{\mathrm{d}\boldsymbol{V}}{\mathrm{d}t} = \hat{\boldsymbol{\xi}}(\dot{u}+qw-rv) + \hat{\boldsymbol{\eta}}(\dot{v}+ru-pw) + \hat{\boldsymbol{\zeta}}(\dot{w}+pv-qu)$$

and

$$\frac{\mathrm{d}\hat{\boldsymbol{\xi}}}{\mathrm{d}t} = \boldsymbol{\omega}\times\hat{\boldsymbol{\xi}} = r\hat{\boldsymbol{\eta}} - q\hat{\boldsymbol{\zeta}}$$

It may be shown that

$$\frac{\mathrm{d}}{\mathrm{d}t}|\boldsymbol{V}| = \frac{1}{|\boldsymbol{V}|}\left(\boldsymbol{V}\cdot\frac{\mathrm{d}\boldsymbol{V}}{\mathrm{d}t}\right)$$

Because

$$\sin\sigma = \frac{\sqrt{v^2+w^2}}{|\boldsymbol{V}|}$$

we finally obtain the rate of change of total incidence angle as

$$\frac{\mathrm{d}\sigma}{\mathrm{d}t} = \frac{[u^2(\dot{u}+qw-rv)+uv(\dot{v}+ru-pw)+uw(\dot{w}+pv-qu)-\dot{u}(u^2+v^2+w^2)]}{|\boldsymbol{V}|^2\sqrt{v^2+w^2}} \tag{3}$$

The axis of rotation is the perpendicular through G to the Λ plane. Using the convention for the positive sense of angular velocities, the vector rate of change of σ is $\hat{\boldsymbol{\sigma}}_d|\mathrm{d}\sigma/\mathrm{d}t|$, where $\hat{\boldsymbol{\sigma}}_d$ is given in Eq. (4).

If the yaw damping moment is now written as $M_q\,\mathrm{d}\sigma/\mathrm{d}t$, the integration of the equations of motion is straightforward and Earth coordinate trajectories and projectile body motions are easily recovered. When it is desired to separate the heave (the $\dot{\boldsymbol{\alpha}}$ motion) and the rotation (the $\boldsymbol{R}$ motion), then the vector rate of change of total incidence must be split into these two contributions. The formulation of this is described in the next section.

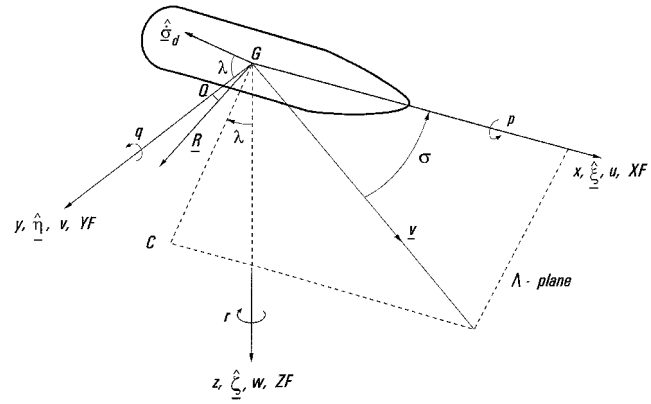

Fig. 1 Body coordinate system and notation.

Components of the Vector Rate of Change of Total Incidence

In Fig. 1, GC is a segment of the line where the Λ plane meets the body y–z plane and $\hat{\boldsymbol{\sigma}}_d$ is the unit vector at G perpendicular to the Λ plane (and so to GC). Therefore, in terms of the unit vectors $\hat{\boldsymbol{\eta}}$ and $\hat{\boldsymbol{\zeta}}$, we have

$$\hat{\boldsymbol{\sigma}}_d = \hat{\boldsymbol{\eta}}\cos\lambda - \hat{\boldsymbol{\zeta}}\sin\lambda \tag{4}$$

Also from Fig. 1, the rotation vector $\boldsymbol{R}$ is representable as

$$\boldsymbol{R} = q\hat{\boldsymbol{\eta}} + r\hat{\boldsymbol{\zeta}} \tag{5}$$

Because in the body y–z plane the vector sum of $\dot{\boldsymbol{\alpha}}$ and $\boldsymbol{R}$ is equal to $\hat{\boldsymbol{\sigma}}_d\,\mathrm{d}\sigma/\mathrm{d}t$, then the projection of $|\boldsymbol{R}|$ onto $\hat{\boldsymbol{\sigma}}_d\,\mathrm{d}\sigma/\mathrm{d}t$ is given by

$$|\boldsymbol{R}|\cos(\lambda+Q) = q\cos\lambda - r\sin\lambda$$

(see Fig. 1). Hence the projection of $\dot{\boldsymbol{\alpha}}$ onto $\hat{\boldsymbol{\sigma}}_d\,\mathrm{d}\sigma/\mathrm{d}t$ has length

$$\frac{\mathrm{d}\sigma}{\mathrm{d}t} - (q\cos\lambda - r\sin\lambda)$$

Now the expression for $\mathrm{d}\sigma/\mathrm{d}t$ in Eq. (3) can be rewritten in the form

$$\frac{\mathrm{d}\sigma}{\mathrm{d}t} = \left[\frac{(u\overline{YF}-v\overline{XF})\sin\lambda + (u\overline{ZF}-w\overline{XF})\cos\lambda}{|\boldsymbol{V}|^2}\right] + q\cos\lambda - r\sin\lambda \tag{6}$$

in which

$$\overline{XF} = XF/m = \dot{u}+qw-rv$$

$$\overline{YF} = YF/m = \dot{v}+ru-pw$$

$$\overline{ZF} = ZF/m = \dot{w}+pv-qu$$

Hence, the projection of $\dot{\boldsymbol{\alpha}}$ onto $\hat{\boldsymbol{\sigma}}_d\,\mathrm{d}\sigma/\mathrm{d}t$ is given by the term in square brackets of Eq. (6). Because $\mathrm{d}\sigma/\mathrm{d}t$ is the length of the vector $(\mathrm{d}\sigma/\mathrm{d}t)\hat{\boldsymbol{\sigma}}_d$, in numerical work the absolute value of the right-hand side of Eq. (6) is used.

Next we consider projections onto the Λ plane. From Fig. 1 the length of the projection of $\boldsymbol{R}$ onto this plane is $|\boldsymbol{R}|\sin(\lambda+Q)$, that is,

$$q\sin\lambda + r\cos\lambda$$

Because $\dot{\boldsymbol{\alpha}}+\boldsymbol{R} = \hat{\boldsymbol{\sigma}}_d\,\mathrm{d}\sigma/\mathrm{d}t$ and $\hat{\boldsymbol{\sigma}}_d$ is perpendicular to the Λ plane, the projections of $\dot{\boldsymbol{\alpha}}$ and $\boldsymbol{R}$ onto this plane are equal in length but of opposite sign.

Therefore along $\hat{\boldsymbol{\sigma}}_d$, $\dot{\boldsymbol{\alpha}}$ has the component

$$\frac{(u\overline{YF} - v\overline{XF})\sin\lambda + (u\overline{ZF} - w\overline{XF})\cos\lambda}{|\boldsymbol{V}|^2} \tag{7}$$

and along the direction $\boldsymbol{GC}$,

$$-(q\sin\lambda + r\cos\lambda) \tag{8}$$

where the direction of $\boldsymbol{GC}$ is given by the unit vector $\hat{\boldsymbol{\eta}}\sin\lambda + \hat{\boldsymbol{\zeta}}\cos\lambda$. Hence

$$\dot{\boldsymbol{\alpha}} = \frac{(\hat{\boldsymbol{\eta}}\cos\lambda - \hat{\boldsymbol{\zeta}}\sin\lambda)}{|\boldsymbol{V}|^2} \times [(u\overline{YF} - v\overline{XF})\sin\lambda + (u\overline{ZF} - w\overline{XF})\cos\lambda] - (q\sin\lambda + r\cos\lambda)(\hat{\boldsymbol{\eta}}\sin\lambda + \hat{\boldsymbol{\zeta}}\cos\lambda) \tag{9}$$

Let

$$\frac{u\overline{YF} - v\overline{XF}}{|\boldsymbol{V}|^2} = A_d$$

and

$$\frac{u\overline{ZF} - w\overline{XF}}{|\boldsymbol{V}|^2} = B_d$$

After some manipulation we find that

$$|\dot{\boldsymbol{\alpha}}| = \sqrt{(A_d\sin\lambda + B_d\cos\lambda)^2 + (q\sin\lambda + r\cos\lambda)^2} \tag{10}$$

Also, in the y–z plane $\dot{\boldsymbol{\alpha}}$ makes an angle S with the body y axis, where

$$\tan S = -\frac{(A_d\sin^2\lambda + B_d\sin\lambda\cos\lambda + q\sin\lambda\cos\lambda + r\cos^2\lambda)}{(A_d\sin\lambda\cos\lambda + B_d\cos^2\lambda - q\sin^2\lambda - r\sin\lambda\cos\lambda)} \tag{11}$$

Finally, using this notation, we can rewrite Eq. (6) as

$$\frac{\mathrm{d}\sigma}{\mathrm{d}t} = A_d\sin\lambda + B_d\cos\lambda + q\cos\lambda - r\sin\lambda \tag{12}$$

The analog of Eq. (6) for angular rates about the pitch axis may be found by repeating the analysis with the projection $\boldsymbol{V}_p = u\hat{\boldsymbol{\xi}} + w\hat{\boldsymbol{\zeta}}$ of $\boldsymbol{V}$ onto the x–z plane instead of $\boldsymbol{V}$ and the angle θ measured from $\boldsymbol{V}_p$ to the body x axis instead of σ. The result is

$$\frac{\mathrm{d}\theta}{\mathrm{d}t} = \frac{1}{|\boldsymbol{V}_p|^2}(u\overline{ZF} - w\overline{XF}) + q$$

which leads to the individual pitch damping coefficients considered in Ref. 2.

Test Cases

To confirm the preceding results, it is required to find motions for which the results are known or for which they can be deduced independently. The examples chosen are suggested by those of Ref. 2; they consist of a motion with body angular rate only, a motion with heave only, and a motion with body spin and with $\dot{\boldsymbol{\sigma}} = \dot{\boldsymbol{\alpha}} = \boldsymbol{R} = 0$.

Loop

The first is a planar loop in the vertical plane with spin rate zero depicted in Fig. 2. For simplicity, gravitational acceleration is assumed absent and there is no force in the body y direction.

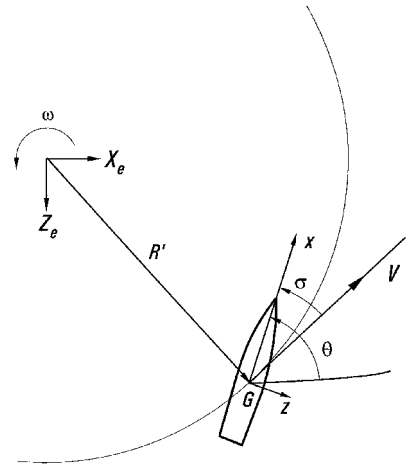

Fig. 2 Loop.

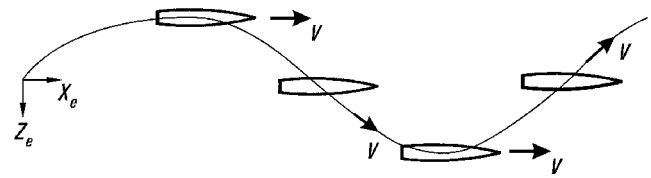

Fig. 3 Motion of spinning projectile in the vertical plane.

To achieve a loop with a fixed total incidence, the body angular rate is equal to the rate of rotation of the line of flight relative to Earth axes, that is, $q = \omega = \mathrm{d}\theta/\mathrm{d}t$. Additionally, $\dot{u}$ and $\dot{w}$ are both identically zero. Writing u as $V\cos\sigma$ and w as $V\sin\sigma$ and v as 0, the terms in Eq. (6) become $\overline{XF} = qV\sin\sigma$, $\overline{ZF} = -qV\cos\sigma$, and $\overline{YF} = 0$.

Next, from Fig. 1, $\tan\lambda = v/w$, so that here $\lambda = 0$ deg; hence Eq. (12) gives $\mathrm{d}\sigma/\mathrm{d}t = 0$, Eq. (4) gives $\hat{\boldsymbol{\sigma}}_d = -\hat{\boldsymbol{\eta}}$, Eq. (9) gives $\dot{\boldsymbol{\alpha}} = -q\hat{\boldsymbol{\eta}}$, and Eq. (5) gives $\boldsymbol{R} = +q\hat{\boldsymbol{\eta}}$.

Alternatively, from Eq. (5), $|\boldsymbol{R}| = q$; because $\tan Q = r/q$ and $r = 0$, we have $Q = 0$; from Eq. (10), $|\dot{\boldsymbol{\alpha}}| = q$, and from Eq. (11), $S = 180$ deg. Thus $\boldsymbol{R}$ and $\dot{\boldsymbol{\alpha}}$ are equal in magnitude and opposite in direction, thereby enabling σ to remain constant in the presence of body rotation.

From simple mechanics, the centripetal force on the body must be $m\omega^2 R'$. In general, it has two constant components, $\overline{ZF} = -mR'\omega^2\cos\sigma$ and $\overline{XF} = mR'\omega^2\sin\sigma$. These are $m\overline{XF}$ and $m\overline{ZF}$, respectively, and $\mathrm{d}\sigma/\mathrm{d}t = 0$, all as deduced independently earlier.

Sinusoidal Heave Motion

This is the purely vertical motion of the body center of gravity shown diagrammatically in Fig. 3; here $u = u_e$ is constant, and the projectile has an axial spin rate p. We derive the required force input in body coordinates to give such a motion and then show that $\dot{\boldsymbol{\alpha}} = \dot{\boldsymbol{\sigma}}$. We have from Fig. 3

$$z_e = z_0\sin pt$$

where pt is equal to the Euler angle ϕ[3].

Now

$$w_e = \frac{\mathrm{d}z_e}{\mathrm{d}t} = z_0 p\cos pt$$

and so

$$Z_e = m\frac{\mathrm{d}^2 z_e}{\mathrm{d}t^2} = -z_0 mp^2\sin pt \tag{13}$$

In fact, Z_e is the only nonzero component of the applied force in Earth-fixed axes because $Y_e = 0$ (motion in vertical plane) and $X_e = 0$ (u_e is constant). Now the body y and z axes are obtained by rotating the y_e and z_e axes clockwise through the angle ϕ (looking

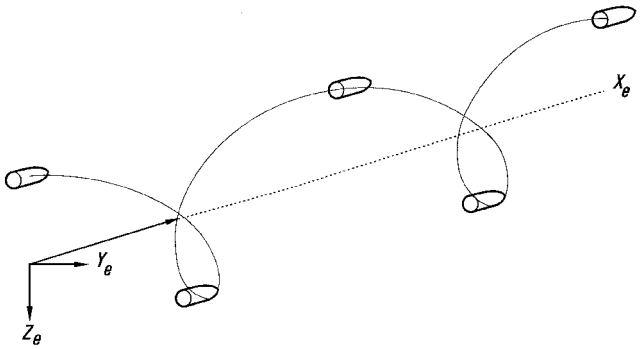

Fig. 4 Lunar motion of projectile.

toward the nose). Hence, by resolving Z_e along these body axes, we obtain

$$YF = z_e \sin\phi = -z_0 mp^2 \sin^2 pt$$

$$ZF = z_e \cos\phi = -z_0 mp^2 \sin pt \cos pt$$

Also, because $\dot{u} = \dot{u}_e = 0$ and $q = r = 0$, we have $XF = 0$.

Then it follows from Eqs. (4), (6), and (9) that $\dot{\boldsymbol{\sigma}} = \dot{\boldsymbol{\alpha}}$.

Helical Motion

In this motion, the center of gravity of the flight vehicle traverses a helical flight path. The longitudinal axis of the vehicle is orientated in the same direction as the axis of the helix but displaced from it by a constant distance. A fixed body axial spin rate equal to the angular rate of rotation of the helical flight path is present. The resulting motion is sometimes referred to as lunar motion because the same surface of the body is always orientated toward the central axis of the maneuver; in aircraft maneuver terminology it is equivalent to a barrel roll. A three-dimensional view of the motion is given in Fig. 4.

Again, with gravity neglected, we can write $u = w = 0$, $\dot{u} = \dot{v} = \dot{w} = 0$, and $q = r = 0$. It follows that $\overline{XF} = \overline{YF} = 0$ and that $\overline{ZF} = pv$. Because λ is now 0 deg, $\mathrm{d}\sigma/\mathrm{d}t$, $\dot{\alpha}$, and R are all zero. This result is again consistent with that predicted by Eqs. (4–6), (10), and (11). Note that, because of the presence of axial spin, this is not the same case as that considered in Ref. 2.

Conclusions

For the six-degree-of-freedommotion of a general rigid body, expressions are derived for the two rotational velocity vectors that are the components of the rate of change of total incidence expressed in terms of quantities defined in body axes. They are presented in a form that is useful for the modeling of the flight of a nonaxisymmetric vehicle. Using them, computations may now be made where explicit values for the individual components of the pitch damping coefficient sum are available.

The fundamental expressions are the magnitude and direction of the rate of change of total incidence, of the component of the body angular rate in the transverse plane through the center of gravity, and of the heave component.

References

[1]Longdon, L. W. (ed.), *Textbook of Ballistics and Gunnery*, Vol. 1, 1st ed., Her Majesty's Stationery Office, London, 1987, p. 451.

[2]Weinacht, P., "Navier–Stokes Predictions of the Individual Components of the Pitch-Damping Coefficient Sum," *Proceedings of the 15th International Symposium on Ballistics* (International Ballistics Committee, Jerusalem, Israel), American Defense Preparedness Association, Arlington, VA, 1995, pp. 339–346 (Paper EB5).

[3]Etkin, B., *Dynamics of Flight—Stability and Control*," 1st ed., Wiley, New York, 1982, p. 47.

J. R. Maus
Associate Editor

Evolution of Secondary Electron Emission Characteristics of Spacecraft Surfaces

R. E. Davies* and J. R. Dennison†
Utah State University, Logan, Utah 84322-4415

Introduction

SECONDARY electron emission (SEE), i.e., the ejection of low-energy (≤50 eV) electrons from surfaces as a result of energetic electron bombardment, is a key process in the electrical charging of spacecraft operating in a wide range of orbital regimes.[1] Although severe charging is most often associated with spacecraft operating at geosynchronous altitudes, greater-than-kilovoltevents have also been reported aboard polar orbiting spacecraft as low as 800 km, and SEE has been identified as one of the dominant mechanisms underlying these events.[2] Myriad operational anomalies, ranging in severity from minor component disruptions, to temporary loss of vehicle control, to, in at least two very expensive instances, the complete loss of an entire spacecraft, are well-documented consequences of the differential charging of spacecraft components[3] and of obvious concern to spacecraft designers and controllers. Spacecraft charging models, such as NASA's NASCAP, NASCAP/LEO, and POLAR codes, have been developed to predict charging levels that a given spacecraft may experience based on its geometry, orbit, and the various materials used in its construction.[3] Critical to the accuracy of these models are estimations of secondary electron (SE) yields, i.e., the numbers of SEs emitted per incident primary electron, for given surfaces under varying conditions of energetic electron bombardment.[1] SE yields are functions of both material and incident electron energy, and the charging codes incorporate these dependencies via empirically derived SEE models—models requiring, as inputs, experimentally determined yield-vs-energy curves for a variety of spacecraft materials.[3] Not presently incorporated into the charging codes, however, are the constantly evolving surface conditions aboard vehicles operating in the space environment, and the effects of such surface evolution on the production of SEs. (These changes result from the continuous removal and addition of surface contaminants as a result of energetic electron, ion, and photon and atomic oxygen bombardment.)

Because SEE is primarily a surface phenomenon, SE yields are extremely sensitive to the presence of surface contaminants such as oxide layers and carbon films. From an SEE standpoint, then, the addition or removal of surface contaminants effectively changes the material, resulting in a (sometimes drastically) changing yield-vs-energy curve. Therefore, as a spacecraft's surfaces evolve, so too do its SEE characteristicsand, consequently, its susceptibility to significant charging in a given environment. Although this fact has been appreciated qualitatively for a number of years,[3] the importance of surface conditions and the dynamic evolution of the surface to charging levels has remained largely uninvestigated and therefore unavailable for incorporation into the charging codes.

The purpose of our investigation, therefore, is twofold: 1) SEE characterization of (conducting) spacecraft materials, subject to varying degrees and types of surface contamination to which operating spacecraft might realistically be subjected and 2) investigation of the dynamic evolution of SE yields resulting from energetic electron and ion bombardment of surfaces within a rarefied atmosphere representative of the microenvironment surrounding space vehicles—a region typically contaminated with the byproducts of maneuvering thrusters and by the outgassing of non-vacuum-compatible materials on and within the spacecraft. This Note reports experimental results that indicate that contamination and surface

Received Jan. 17, 1997; revision received May 14, 1997; accepted for publication May 14, 1997.

*Graduate Research Assistant, Department of Physics, UMC 4415.

†Associate Professor, Department of Physics, UMC 4415.